Maritime NO_x Emissions Over Chinese Seas Derived From Satellite Observations

Ding, J.; Johannes Van Der A, Ronald; Mijling, B; Jalkanen, J. P.; Johansson, L; Levelt, P. F.

DOI
10.1002/2017GL076788

Publication date
2018

Document Version
Final published version

Published in
Geophysical Research Letters

AGU PUBLICATIONS

Geophysical Research Letters

RESEARCH LETTER
10.1002/2017GL076788

Key Points:
- Satellite-derived NO_x emissions from maritime sources for 10 years over Chinese seas
- The decadal trend of NO_x emissions over Chinese seas is analyzed for the first time
- The impact of shipping emissions on air quality in coastal regions is significant

Correspondence to:
J. Ding,
jieying.ding@knmi.nl

Citation:
Ding, J., van der A, R. J., Mijling, B., Jalkanen, J.-P., Johansson, L., & Levelt, P. F. (2018). Maritime NO_x emissions over Chinese seas derived from satellite observations. *Geophysical Research Letters*, *45*, 2031–2037. https://doi.org/10.1002/2017GL076788

Received 18 DEC 2017
Accepted 3 FEB 2018
Accepted article online 7 FEB 2018
Published online 20 FEB 2018

Maritime NO_x Emissions Over Chinese Seas Derived From Satellite Observations

J. Ding[1,2], R. J. van der A[1], B. Mijling[1], J.-P. Jalkanen[3], L. Johansson[3], and P. F. Levelt[1,2]

[1]R&D Satellite Observations, Royal Netherlands Meteorological Institute (KNMI), De Bilt, Netherlands, [2]Department of Geoscience and Remote Sensing, Delft University of Technology, Delft, Netherlands, [3]Atmospheric Composition Research, Finnish Meteorological Institute, Helsinki, Finland

Abstract By applying an inversion algorithm to NO_x satellite observations from Ozone Monitoring Instrument, monthly NO_x emissions for a 10 year period (2007 to 2016) over Chinese seas are presented for the first time. No effective regulations on NO_x emissions have been implemented for ships in China, which is reflected in the trend analysis of maritime emissions. The maritime emissions display a continuous increase rate of about 20% per year until 2012 and slow down to 3% after that. The seasonal cycle of shipping emissions has regional variations, but all regions show lower emissions during winter. Simulations by an atmospheric chemistry transport model show a notable influence of maritime emissions on air pollution over coastal areas, especially in summer. The satellite-derived spatial distribution and the magnitude of maritime emissions over Chinese seas are in good agreement with bottom-up studies based on the Automatic Identification System of ships.

Plain Language Summary This paper presents NOx emissions derived from satellite observations over the Chinese seas for the last 10 years. The maritime emissions have a continuous increase rate of about 20% per year until 2012 and slow down to about 3% afterward. This reflects that almost no effective regulations on NOx emissions have been implemented for ships in China. The impact of maritime emissions on air quality over coastal areas in China is significant as shown by simulations using a chemical transport model.

1. Introduction

NO_x ($NO_x = NO_2 + NO$) emissions from oceangoing ships contribute more than 10% of the total anthropogenic NO_x emissions worldwide (Corbett et al., 1999). They have a large impact on the atmospheric chemistry and air quality in the marine boundary layer and consequently have an impact on climate change (Eyring et al., 2010; Lawrence & Crutzen, 1999) and human health (H. Liu et al., 2016). Furthermore, the aerosol particles from ships may affect the maritime deep convection. This could lead to enhanced lightning and therefore additional NO_x formation over shipping lanes (Thornton et al., 2017). Maritime transport emissions have large uncertainties due to the difficulty in determining shipping activities and emission factors. Fortunately, satellite observations of NO_2 provide the possibility to detect ship tracks and estimate emissions. Beirle et al. (2004) showed the first detection of NO_x ship emissions derived by satellite observations of GOME over the Indian ocean by fitting the observations with a Gaussian function. Richter et al. (2004) found a clear NO_2 signal over the Red Sea and the Indian Ocean using the observations from the SCanning Imaging Absorption spectroMeter for Atmospheric CHartographY instrument. Furthermore, the combination of satellite observations with modeled columns of a chemical transport model (CTM) can be used to evaluate NO_x emissions in ship tracks. This was, for instance, used by Franke et al. (2009) to estimate the total NO_x emissions along the ship track from Sri Lanka to Indonesia. By using a mass balance approach applied to the high spatial resolution measurements from the Ozone Monitoring Instrument (OMI) (Levelt et al., 2006), Vinken et al. (2014) derived shipping emission estimates over parts of the European seas. Note that all mentioned methods are only applicable for specific ship tracks far away from sources over land. The NO_x emissions from shipping activities are difficult to detect from space near Chinese coastal areas since the ship tracks are hidden in the outflow of NO_2 plumes from the mainland (see Figure 1a). Traditional ship inventories are often lacking information on these ship activities or have large uncertainties on their ship emissions (C. Wang et al., 2008; Y. Zhang et al., 2017). Ding et al. (2017) showed clear satellite-derived NO_x emissions near Chinese coastal areas by using the inversion algorithm DECSO (Daily Emission estimates Constrained from Satellite Observations) combining CTM simulations and OMI satellite observations.

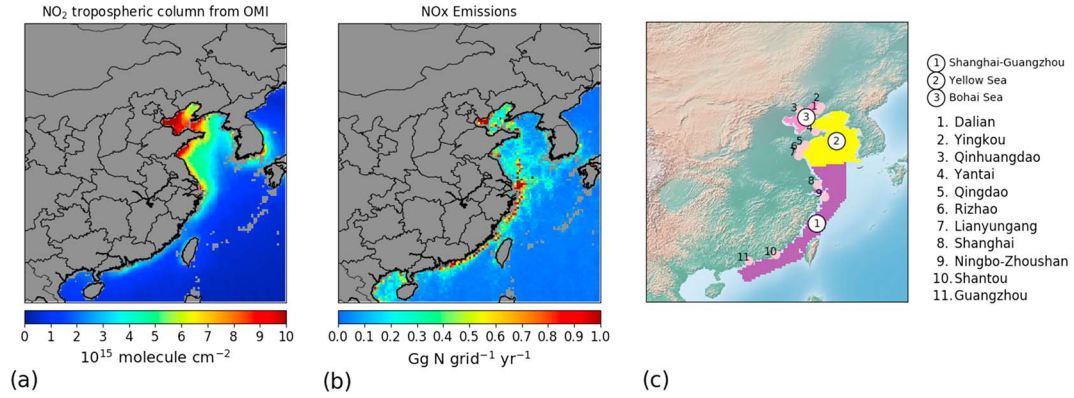

Figure 1. The average of (a) tropospheric NO_2 column concentrations over ocean observed by Ozone Monitoring Instrument (OMI) from 2007 to 2016 and (b) NO_x emissions over ocean derived by Daily Emission estimates Constrained from Satellite Observations applied to these OMI observations. (c) The three selected regions to study the shipping emissions near the Chinese coast are shown as colored areas. The numbers in the circle indicate the name of the regions. The numbers on the coasts indicate the locations of the main harbors.

In the last decade, seaborne trade increased rapidly in East Asia. The number of studies of shipping emissions on a regional scale in East Asia is limited, and most of them are at port or city level (Y. Zhang et al., 2017). The application of the data from the Automatic Identification System (AIS) significantly reduced uncertainties in bottom-up shipping emission inventories (Jalkanen et al., 2009). Fan et al. (2016) build an AIS-based model to calculate high-resolution shipping emissions of 2010 in the sea around the Chinese Yangtze River Delta and parts of the East China Sea. Using a similar method, H. Liu, Fu, et al. (2016) estimated that shipping emissions in East Asia accounted for 16% of the global shipping emissions in 2013. They also found that shipping emissions of NO_x in this region almost doubled compared to emissions in 2001.

Based on the long-term record of NO_2 satellite observations from OMI, this study presents maritime NO_x emissions from 2007 to 2016 over the Chinese seas using DECSO. The long and consistent data series allows us to analyze the seasonal cycle and the trend of maritime NO_x emissions over Chinese seas. Since few air quality regulations on NO_x have been taken for maritime transport in China, a persistent increase in shipping emissions is expected following the trend in cargo trade volumes. The effect of maritime emissions on NO_2 concentrations in coastal cities is investigated by using a regional CTM. To validate the results, the emissions are compared with the latest bottom-up ship emission inventory based on AIS data derived with the Ship Traffic Emission Assessment Model (STEAM) (Jalkanen et al., 2016).

2. Emission Estimates

Daily Emission estimates Constrained from Satellite Observations is a fast inverse modeling algorithm developed by Mijling and van der A (2012) to update daily emissions of NO_x based on an extended Kalman filter. The algorithm combines simulated NO_2 column concentrations of a regional CTM with satellite observations. The sensitivity of NO_2 column concentrations on local and nonlocal NO_x emissions is calculated by including a simplified isobaric surface 2-D trajectory analysis. The improvements in the latest version of DECSO (referred to as DECSO v5) by Ding et al. (2017) enabled the detection of ship tracks near the Chinese coasts by significantly reducing the background noise of estimated NO_x emissions over remote areas.

We derived NO_x emissions over Chinese seas in the domain of East Asia (102–120°E, 18–50°N) with a horizontal resolution of 0.25° × 0.25° from 2007 to 2016 by using DECSO v5. The Eulerian regional off-line CTM CHIMERE v2013 (Menut et al., 2013) is used to simulate NO_2 concentrations. Its implementation in DECSO is described in Ding et al. (2015). The a priori emission field over the ocean is set to zero. We set the injection height of newly found emissions over oceans at 40 m, representing an average funnel height for ships. We apply DECSO to observations from OMI due to its high spatial resolution, which is 24 × 13 km^2 at nadir and increases to 150 × 28 km^2 at the end of the swath. The tropospheric NO_2 column data of the DOMINO version 2 algorithm (Boersma et al., 2011) are used for the assimilation. To ensure retrievals in good

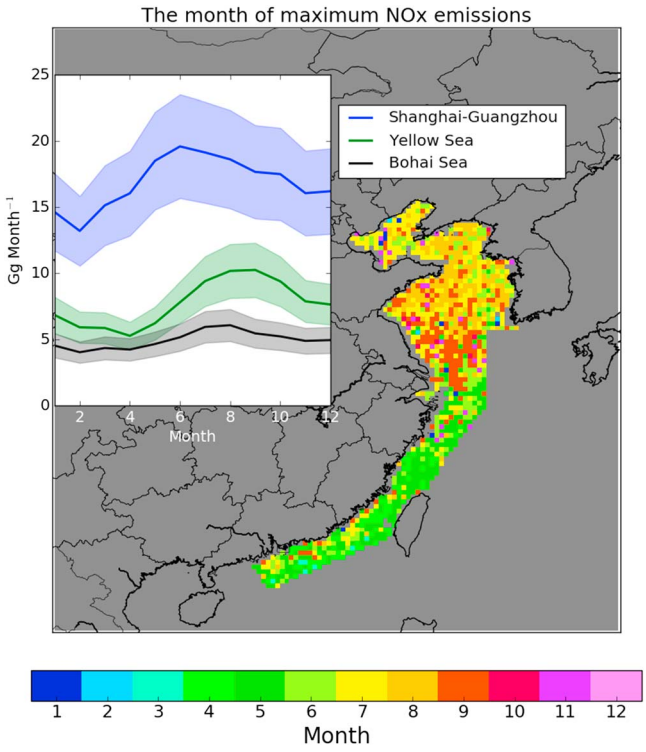

Figure 2. The month with the maximum monthly NO_x emissions for each grid cell over the ocean. The inset figure is the seasonal cycle of NO_x emissions for the selected three areas shown in Figure 1c. The shaded bands in the inset figure indicate the uncertainty.

quality, we use the filter criteria described by Ding et al. (2015, 2017) on the retrievals. In addition, to detect clear ship tracks, we exclude the observations with a large pixel size by filtering out 8 pixels at each side of the swath. The observations with a cloud radiance fraction larger than 50% are excluded.

We use monthly NO_x emissions for our analysis. To calculate the uncertainty of monthly emissions in each region, we use the daily error estimate on each grid cell from the Kalman filter, which propagates errors from observations and the model. We assume that the error of each grid cell has high temporal (day to day) correlation (up to 90%) but low spatial correlation with an upper limit of 20% with the eight neighboring grid cells.

3. Results

Figure 1b shows the average annual NO_x emissions from 2007 to 2016 derived with DECSO v5 over the Chinese seas. We see a clear ship track along the coast between Shanghai and Guangzhou. Over the Yellow Sea, high shipping emissions are revealed near Jiangsu province. A track from Shanghai to Yantai disperses in the Bohai Sea. We see high maritime emissions over the Bohai Sea and around the ports of Shanghai and Guangzhou. Half of the Chinese offshore platforms are located in the Bohai Sea. Over remote ocean areas, NO_x emissions are much lower and no notable shipping tracks are visible due to the low density of shipping activities, as confirmed by real-time shipping locations from AIS. Most shipping activities occur close to the coastal areas. Ding et al. (2017) depicted the shipping emissions derived with DECSO near the coastline and concluded that their spatial distribution is consistent with the density of shipping activities. In this paper, we analyze the seasonal cycle and trends of maritime emissions resulting from ships and offshore platforms in this area. We classify three regions shown in Figure 1c, to study the evolution of shipping emissions near the Chinese coast.

3.1. Seasonal Cycle

In Figure 2, the month with the maximum monthly NO_x emissions for each grid cell over the ocean together with the seasonal cycle over each region are illustrated. The upper limit of the relative error of the 10 year averaged monthly emissions per region is estimated to be about 20%. A clear pattern of the maximum month distribution is visible over the Chinese seas. This means that the seasonal cycles of the shipping emissions have regional variation. Shipping emissions reach a maximum in May over southern Chinese seas. More northward, over the Yellow Sea and the Bohai Sea, the monthly shipping emissions gradually reach their maximum later. This can be explained by the start of summer monsoon in mid-May over southern Chinese seas, which moves steadily northwards over East China (Burke & Stott, 2017). J. Wang et al. (2014) showed that the monsoonal climate and tropical cyclones decrease the safety for ships in the South China Sea, which results in fewer ships after May. Besides the influence of weather, the different summer moratorium of fishing in these areas is possibly another reason for the difference in the peak month of emissions. Over the Yellow Sea, shipping emissions increase in summer, which might be explained by the increase of tourism activities, while the shipping emissions reach their peak in September, because more fishing ships are expected in this month after the lifting of the summer moratorium in this area (Shen & Heino, 2014). Over the Bohai Sea and the Yellow Sea especially, the shipping activities decrease in winter due to sea ice and bad weather and start to increase again in April (L. Wang et al., 2013; F. Zhang et al., 2014).

3.2. Trend Analysis

Figure 3a shows the linear change rate of shipping emissions in each grid cell from 2007 to 2016. We see a clear increasing trend at the track along the southern coast from Guangzhou to Shanghai and continuing to Shandong Province in the Yellow Sea with an average increase rate of about 0.1 Gg per grid cell per year.

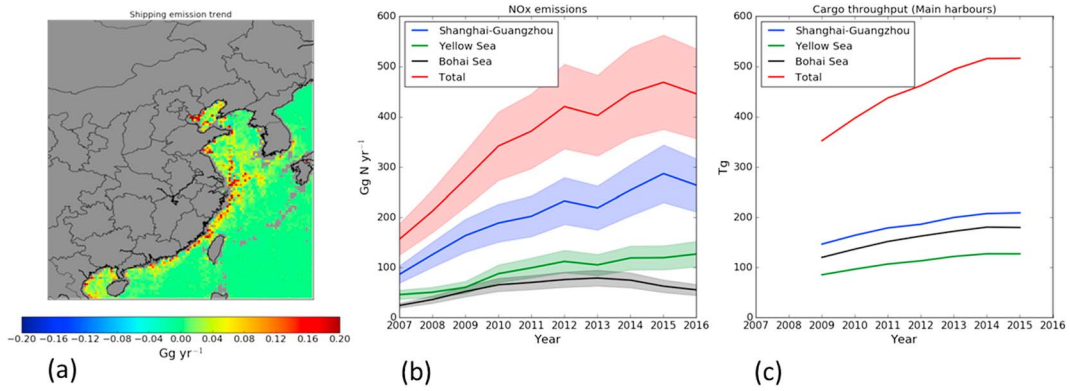

Figure 3. (a) The linear change rate of NO_x emissions per grid cell over the ocean from 2007 to 2016. The time series of (b) NO_x emissions from 2007 to 2016 and (c) cargo throughput volumes from main harbors from 2009 to 2015 over the selected three regions shown in Figure 1c. The shaded bands in (b) indicate the uncertainty.

Figure 4 shows the annual shipping emissions with an estimated uncertainty of about ±20% for each of the selected three regions. We see that the relative increase rate levels off progressively, from about 30% per year in 2007 to a very small trend in the last years. We have currently no explanation for the decrease in 2013 and 2016. This is quite different compared to the trend of NO_x emissions and columns over Mainland China, where the NO_x emissions started to decrease since 2012 (F. Liu et al., 2016; van der A et al., 2017).

To rationalize the trend shown in Figure 3b, we obtain the annual cargo throughput data of the main harbors (shown in Figure 1c) along the coast for the period of 2009 to 2015 from the National Bureau of Statistics China (2017). Cargo throughput volumes are commonly regarded as an indicator for shipping emissions (Streets et al., 1997) and used to compare with trends (de Ruyter de Wildt et al., 2012). Note that this does not account for fishing ships, recreational ships, and for the size of cargo ships. Figure 3c shows that the total volume of cargo throughput increased between 2009 and 2014 after which it remained at the same level. The trend is similar to that of shipping emissions shown in Figure 3b. Both emissions and cargo throughput show an increase of about 40% in 2012 compared to 2009. The ports along the Bohai Sea, Yellow Sea, and the region from Shanghai to Guangzhou are summed up separately to approximate the shipping activity for these three regions. Note that ships delivering their cargo in ports of one region (especially Bohai) often also pass the other regions. For the Yellow Sea, this explains the lower cargo throughput compared to the higher NO_x emissions. The correlation coefficient (R) of the time series between shipping emissions and cargo

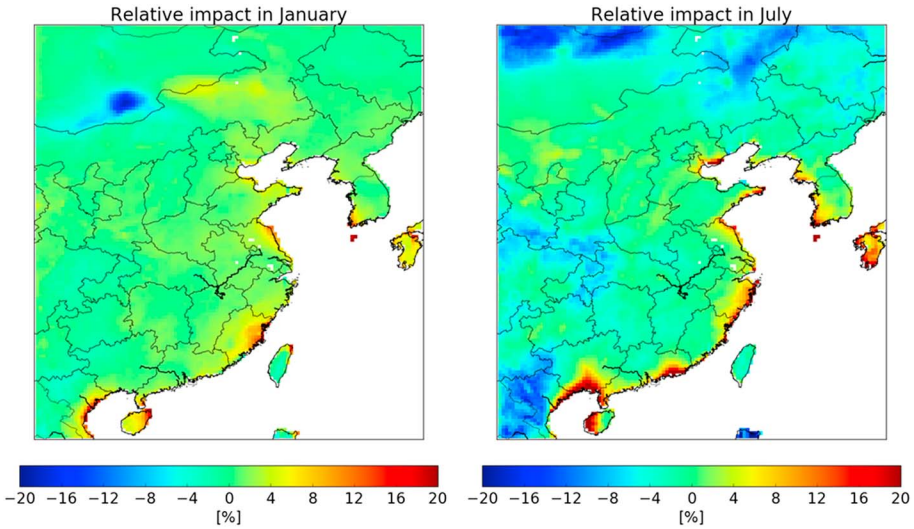

Figure 4. The relative impact of maritime emissions on the NO_2 columns over land in January and July 2015.

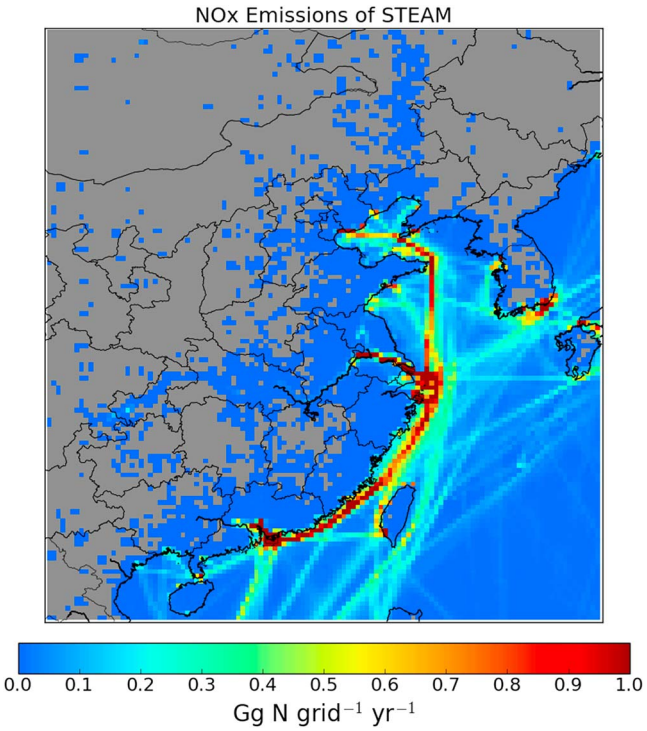

Figure 5. Shipping emissions derived from the Ship Traffic Emission Assessment Model using Automatic Identification System data in 2015.

throughput volumes are all above 0.95, for the Yellow sea, Shanghai-Guangzhou, and the total of three regions, except for the Bohai Sea, which has an *R* value of 0.84. We see that the annual emissions over the Bohai Sea show a decrease starting in 2014, while the cargo throughput volume becomes stable. Note that the emissions derived with DECSO are the total surface emissions. Over the Bohai Sea, the total NO_x emissions include the emissions not only from ships but also from several oil platforms in this region (Xing et al., 2015). In 2014, oil companies and the government signed the document "Responsibility for the total emission reduction targets" (Ren & Jin, 2014), in which the companies promise to reduce air pollutants from marine oil platforms. This might explain the decrease of emissions over the Bohai Sea after 2014. For all three regions, we see that the increase rate of emissions is higher than that of cargo throughput. This implies that regulations on NO_x emissions are either inexistent or ineffective for the maritime sector over open seas.

3.3. Contribution of Shipping Emissions to NO_2 Air Pollution

Shipping emissions near coastal areas amount to about 10% of the total emissions over the mainland in our study domain. To study the influence of shipping emissions on shore regions, we set up two CHIMERE runs for the year 2015: one run using the MIX inventory (Li et al., 2017), which includes no maritime emissions, and the other using a combination of the MIX inventory and the maritime emissions of DECSO. We exclude the maritime emissions over the grid cells with more than 5% covering land due to the difficulty in distinguishing them from other sources over land. This will result in an underestimation of the contribution of maritime emissions. From the model results, we see that the shipping lanes near the coast are always covered by the outflow from the mainland. The difference in NO_2 columns between the two runs is regarded as the contribution from shipping emissions. The contribution is higher in summer than in winter due to the summer monsoon wind from ocean to land (see Figure 4). In summer, the maximum occurred at the coastal areas of Fujian and Guangzhou Provinces and the contribution can be as high as 20%. In winter, the contribution from shipping emissions to coastal cities is smaller. The nonnegligible effect of shipping emissions can lead to large uncertainties in model simulations using emission inventories without the maritime sector.

4. Discussion

To further validate our shipping emissions, we compare them with the emissions derived with the STEAM model (Jalkanen et al., 2016), which uses the AIS data worldwide. Data for the Asian region are available only for the year 2015. The resolution of STEAM data is 10 × 10 km. For a meaningful comparison, we regrid the data set to the same resolution as used by DECSO. Figure 5 shows the regridded shipping emission map of STEAM. We see that DECSO (Figure 1b) is in fairly good agreement with STEAM for shipping emissions with strength higher than 0.4 Gg per grid cell per year. However, shipping lanes with limited ship traffic are not visible in the DECSO data, because the resolution of DECSO emissions is limited to the pixel size of satellite observations. The coarse resolution of model and satellite observations can lead to an underestimation of shipping emissions (Valin et al., 2011). The longer lifetime of NO_2 and fewer observations in winter (about half the number of the observations in summer) also lead to larger uncertainties in allocating emissions in DECSO. STEAM has uncertainties because of errors in the emission factor and incomplete AIS data. We calculate the annual emissions of STEAM data for the selected three regions. In 2015, over the Bohai Sea, Yellow Sea, and Shanghai-Guangzhou regions, the annual detected total surface emissions are 23, 84, and 215 Gg with STEAM, while they are respectively 63, 120, and 287 Gg derived with DECSO. A fair agreement is found over the Yellow Sea and the Chinese coastal region between Shanghai and Guangzhou. Over the Bohai Sea area, the emissions of DECSO are much higher than those of STEAM. However, since DECSO is estimating total

emissions over sea, including ships without AIS and emissions from marine oil platforms, which are frequent in this region, emissions of DECSO are expected to be higher here.

The shipping emissions derived with DECSO are also comparable with other recent studies. Fan et al. (2016) used the AIS data to estimate shipping emissions in 2010 near the Yangtze River Delta. The results showed that annual shipping emissions in a zone between 100 and 200 km of the coastline are 150 Gg and in the zone of 200 and 300 km shipping emissions are 63 Gg. Over the same areas, the emissions of DECSO are 143 and 71 Gg, respectively, which is within a 10% error margin. H. Liu, Fu, et al. (2016) derived shipping emissions from AIS data over Chinese seas in 2013, which were about 1,799 Gg per year for the Chinese coastal seas. For the same region, our estimated emissions are about 1,422 Gg. Note that the maritime emissions of DECSO exclude grid cells containing even a small fraction of land. Since these studies for different areas and different years are consistent with emissions from DECSO, these comparisons give us more confidence in our derived emissions and trend analysis.

5. Conclusions

In this study, we present the first long-term record of satellite-derived emissions over Chinese seas by using the DECSO algorithm. DECSO is able to detect total surface emissions under the strong outflow of NO_2 from Mainland China and can be applied to any other region of the world. The emissions are coming from offshore platforms and all motorized ships. The continually increasing trend of NO_x emissions over sea is in agreement with the fact that no effective regulations have been implemented for ships in China. Our model simulations show that shipping emissions can contribute up to 5–20% to local NO_2 concentrations at the densely populated coast. Since data about shipping emissions over China are usually not available, the air quality simulations and forecasts suffer large uncertainties especially near coast areas. DECSO provides monthly emissions for the last 10 years, which provides missing information of emissions over ocean to modelers. In the future, when better satellite observations become available that have higher temporal and spatial resolutions, for example, TROPOspheric Monitoring Instrument (Veefkind et al., 2012) on a Sun-synchronous satellite and geostationary satellites with instruments like Geostationary Environment Monitoring Spectrometer (Kim, 2012) over Asia, Sentinel-4 (Ingmann et al., 2012) over Europe, and TEMPO (Zoogman et al., 2017) over America, we expect to detect even NO_x emissions of low-density ship tracks from space and subsequently to further improve shipping emission inventories.

Acknowledgments
The research was part of the OMI project funded and supported by the Netherlands Space Office. We acknowledge IPSL/LMD, INERIS, and IPSL/LISA in France for providing the CHIMERE model. The NO_x emission data of DECSO are available on www.globemission.eu. The NO_x emission data of STEAM are available on www.globemission.eu/steam/steam.php.

References

Beirle, S., Platt, U., von Glasow, R., Wenig, M., & Wagner, T. (2004). Estimate of nitrogen oxide emissions from shipping by satellite remote sensing. *Geophysical Research Letters*, *31*, L18102. https://doi.org/10.1029/2004GL020312

Boersma, K. F., Eskes, H. J., Dirksen, R. J., van der A, R. J., Veefkind, J. P., Stammes, P., et al. (2011). An improved tropospheric NO_2 column retrieval algorithm for the Ozone Monitoring Instrument. *Atmospheric Measurement Techniques*, *4*(9), 1905–1928. https://doi.org/10.5194/amt-4-1905-2011

Burke, C., & Stott, P. (2017). Impact of anthropogenic climate change on the East Asian Summer Monsoon. *Journal of Climate*, *30*(14), 5205–5220. https://doi.org/10.1175/jcli-d-16-0892.1

Corbett, J. J., Fischbeck, P. S., & Pandis, S. N. (1999). Global nitrogen and sulfur inventories for oceangoing ships. *Journal of Geophysical Research*, *104*, 3457–3470. https://doi.org/10.1029/1998JD100040

de Ruyter de Wildt, M., Eskes, H., & Boersma, K. F. (2012). The global economic cycle and satellite-derived NO2 trends over shipping lanes. *Geophysical Research Letters*, *39*, L01802. https://doi.org/10.1029/2011GL049541

Ding, J., van der A, R. J., Mijling, B., & Levelt, P. F. (2017). Space-based NOx emission estimates over remote regions improved in DECSO. *Atmospheric Measurement Techniques*, *10*(3), 925–938. https://doi.org/10.5194/amt-10-925-2017

Ding, J., van der A, R. J., Mijling, B., Levelt, P. F., & Hao, N. (2015). NO_x emission estimates during the 2014 Youth Olympic Games in Nanjing. *Atmospheric Chemistry and Physics*, *15*(16), 9399–9412. https://doi.org/10.5194/acp-15-9399-2015

Eyring, V., Isaksen, I. S. A., Berntsen, T., Collins, W. J., Corbett, J. J., Endresen, O., et al. (2010). Transport impacts on atmosphere and climate: Shipping. *Atmospheric Environment*, *44*(37), 4735–4771. https://doi.org/10.1016/j.atmosenv.2009.04.059

Fan, Q., Zhang, Y., Ma, W., Ma, H., Feng, J., Yu, Q., et al. (2016). Spatial and seasonal dynamics of ship emissions over the Yangtze River Delta and East China Sea and their potential environmental influence. *Environmental Science & Technology*, *50*(3), 1322–1329. https://doi.org/10.1021/acs.est.5b03965

Franke, K., Richter, A., Bovensmann, H., Eyring, V., Jöckel, P., Hoor, P., & Burrows, J. P. (2009). Ship emitted NO2 in the Indian Ocean: Comparison of model results with satellite data. *Atmospheric Chemistry and Physics*, *9*(19), 7289–7301. https://doi.org/10.5194/acp-9-7289-2009

Ingmann, P., Veihelmann, B., Langen, J., Lamarre, D., Stark, H., & Courrèges-Lacoste, G. B. (2012). Requirements for the GMES atmosphere service and ESA's implementation concept: Sentinels-4/-5 and -5p. *Remote Sensing of Environment*, *120*, 58–69. https://doi.org/10.1016/j.rse.2012.01.023

Jalkanen, J. P., Brink, A., Kalli, J., Pettersson, H., Kukkonen, J., & Stipa, T. (2009). A modelling system for the exhaust emissions of marine traffic and its application in the Baltic Sea area. *Atmospheric Chemistry and Physics*, *9*(23), 9209–9223. https://doi.org/10.5194/acp-9-9209-2009

Jalkanen, J. P., Johansson, L., & Kukkonen, J. (2016). A comprehensive inventory of ship traffic exhaust emissions in the European sea areas in 2011. *Atmospheric Chemistry and Physics*, *16*(1), 71–84. https://doi.org/10.5194/acp-16-71-2016

Kim, J. (2012). GEMS (Geostationary Environment Monitoring Spectrometer) onboard the GeoKOMPSAT to monitor air quality in high temporal and spatial resolution over Asia-Pacific region. Paper presented at the EGU, Vienna, Austria.

Lawrence, M. G., & Crutzen, P. J. (1999). Influence of NOx emissions from ships on tropospheric photochemistry and climate. *Nature*, *402*(6758), 167–170. https://doi.org/10.1038/46013

Levelt, P. F., van den Oord, G. H. J., Dobber, M. R., Malkki, A., Huib, V., de Vries, J., et al. (2006). The Ozone Monitoring Instrument. *IEEE Transactions onGeoscience and Remote Sensing*, *44*(5), 1093–1101. https://doi.org/10.1109/TGRS.2006.872333

Li, M., Zhang, Q., Kurokawa, J. I., Woo, J. H., He, K., Lu, Z., et al. (2017). MIX: A mosaic Asian anthropogenic emission inventory under the international collaboration framework of the MICS-Asia and HTAP. *Atmospheric Chemistry and Physics*, *17*(2), 935–963. https://doi.org/10.5194/acp-17-935-2017

Liu, F., Zhang, Q., van der A, R. J., Zheng, B., Tong, D., Yan, L., et al. (2016). Recent reduction in NOx emissions over China: Synthesis of satellite observations and emission inventories. *Environmental Research Letters*, *11*(11), 114002. https://doi.org/10.1088/1748-9326/11/11/114002

Liu, H., Fu, M., Jin, X., Shang, Y., Shindell, D., Faluvegi, G., et al. (2016). Health and climate impacts of ocean-going vessels in East Asia. *Nature Climate Change*. https://doi.org/10.1038/nclimate3083

Menut, L., Bessagnet, B., Khvorostyanov, D., Beekmann, M., Blond, N., Colette, A., et al. (2013). CHIMERE 2013: A model for regional atmospheric composition modelling. *Geoscientific Model Development*, *6*(4), 981–1028. https://doi.org/10.5194/gmd-6-981-2013

Mijling, B., & van der A, R. J. (2012). Using daily satellite observations to estimate emissions of short-lived air pollutants on a mesoscopic scale. *Journal of Geophysical Research*, *117*, D17302. https://doi.org/10.1029/2012JD017817

Ren, K., & Jin, Y. (2014). Chinese offshore platforms take responsibility in Air Quality Control (in Chinese). Retrieved from http://zhaobiao.cnooc.com.cn/data/html/news/2014-01-09/english/350399.html

Richter, A., Eyring, V., Burrows, J. P., Bovensmann, H., Lauer, A., Sierk, B., & Crutzen, P. J. (2004). Satellite measurements of NO_2 from international shipping emissions. *Geophysical Research Letters*, *31*, L23110. https://doi.org/10.1029/2004GL020822

Shen, G., & Heino, M. (2014). An overview of marine fisheries management in China. *Marine Policy*, *44*, 265–272. https://doi.org/10.1016/j.marpol.2013.09.012

Streets, D. G., Carmichael, G. R., & Arndt, R. L. (1997). Sulfur dioxide emissions and sulfur deposition from international shipping in Asian waters. *Atmospheric Environment*, *31*(10), 1573–1582. https://doi.org/10.1016/S1352-2310(96)00204-X

Thornton, J. A., Virts, K. S., Holzworth, R. H., & Mitchell, T. P. (2017). Lightning enhancement over major oceanic shipping lanes. *Geophysical Research Letters*, *44*, 9102–9111. https://doi.org/10.1002/2017GL074982

Valin, L. C., Russell, A. R., Hudman, R. C., & Cohen, R. C. (2011). Effects of model resolution on the interpretation of satellite NO_2 observations. *Atmospheric Chemistry and Physics*, *11*(22), 11,647–11,655. https://doi.org/10.5194/acp-11-11647-2011

van der A, R. J., Mijling, B., Ding, J., Koukouli, M. E., Liu, F., Li, Q., et al. (2017). Cleaning up the air: Effectiveness of air quality policy for SO2 and NOx emissions in China. *Atmospheric Chemistry and Physics*, *17*(3), 1775–1789. https://doi.org/10.5194/acp-17-1775-2017

Veefkind, J. P., Aben, I., McMullan, K., Förster, H., de Vries, J., Otter, G., et al. (2012). TROPOMI on the ESA Sentinel-5 precursor: A GMES mission for global observations of the atmospheric composition for climate, air quality and ozone layer applications. *Remote Sensing of Environment*, *120*, 70–83. https://doi.org/10.1016/j.rse.2011.09.027

Vinken, G. C. M., Boersma, K. F., van Donkelaar, A., & Zhang, L. (2014). Constraints on ship NO_x emissions in Europe using GEOS-Chem and OMI satellite NO_2 observations. *Atmospheric Chemistry and Physics*, *14*(3), 1353–1369. https://doi.org/10.5194/acp-14-1353-2014

Wang, C., Corbett, J. J., & Firestone, J. (2008). Improving spatial representation of global ship emissions inventories. *Environmental Science & Technology*, *42*(1), 193–199. https://doi.org/10.1021/es0700799

Wang, J., Li, M., Liu, Y., Zhang, H., Zou, W., & Cheng, L. (2014). Safety assessment of shipping routes in the South China Sea based on the fuzzy analytic hierarchy process. *Safety Science*, *62*, 46–57. https://doi.org/10.1016/j.ssci.2013.08.002

Wang, L., Qi, J. H., Shi, J. H., Chen, X. J., & Gao, H. W. (2013). Source apportionment of particulate pollutants in the atmosphere over the Northern Yellow Sea. *Atmospheric Environment*, *70*, 425–434. https://doi.org/10.1016/j.atmosenv.2012.12.041

Xing, Q., Meng, R., Lou, M., Bing, L., & Liu, X. (2015). Remote sensing of ships and offshore oil platforms and mapping the marine oil spill risk source in the Bohai Sea. *Aquatic Procedia*, *3*, 127–132. https://doi.org/10.1016/j.aqpro.2015.02.236

Zhang, F., Chen, Y., Tian, C., Wang, X., Huang, G., Fang, Y., & Zong, Z. (2014). Identification and quantification of shipping emissions in Bohai rim, China. *Science of the Total Environment*, *497–498*, 570–577. https://doi.org/10.1016/j.scitotenv.2014.08.016

Zhang, Y., Yang, X., Brown, R., Yang, L., Morawska, L., Ristovski, Z., et al. (2017). Shipping emissions and their impacts on air quality in China. *Science of the Total Environment*, *581–582*, 186–198. https://doi.org/10.1016/j.scitotenv.2016.12.098

Zoogman, P., Liu, X., Suleiman, R. M., Pennington, W. F., Flittner, D. E., Al-Saadi, J. A., et al. (2017). Tropospheric emissions: Monitoring of pollution (TEMPO). *Journal of Quantitative Spectroscopy and Radiative Transfer*, *186*, 17–39. https://doi.org/10.1016/j.jqsrt.2016.05.008